Dry sliding wear behavior of A356/Al$_2$O$_3$ metal matrix nanocomposites (MMNCs)

E.Y.El-Kady, T.S.Mahmoud*, M.Abdel-Aziz

Mechanical Engineering Department, Faculty of Engineering, King Khalid University (KKU),
Abha, (KINGDOM OF SAUDI ARABIA)

Received: 18th April, 2012 ; Accepted: 4th September, 2012

ABSTRACT

The aim of the present work is to study the dry sliding wear behaviour of A356/Al$_2$O$_3$ nanocomposites at both room and elevated temperatures. Dry wear tests were conducted at several sliding speeds at room temperature. Wear test results showed that The A356/Al$_2$O$_3$ nanocomposites exhibited lower wear rates at both room and elevated temperatures when compared with the A356 monolithic alloy. Increasing the volume fraction and/or reducing the Al$_2$O$_3$ nanoparticles size reduces the wear rates of the A356/Al$_2$O$_3$ nanocomposites. Introducing the Al$_2$O$_3$ nanoparticulates to the A356 aluminum alloy assisted in increasing the mild-to-sever wear transition temperature. The composites exhibited transition temperature between 150 and 200 ℃, while the unreinforced alloy exhibited a transition temperature between 100 and 150 ℃.   © 2013 Trade Science Inc. - INDIA

INTRODUCTION

Metal matrix composites (MMCs) have been extensively studied in last two decades and are significant for numerous applications in the aerospace, automobile, and military industries[1,2]. MMC consists of a metallic base with a reinforcing constituent, usually ceramic. The attractive physical and mechanical properties that can be obtained with MMCs include high specific modulus, superior strength, long fatigue life, high wear resistance, high creep and improved thermal stability. Normally, micro-sized ceramic particles are used to improve the yield and ultimate strength of the metal. However, the ductility of the MMCs deteriorates with high ceramic particle concentration[3]. Recently, it is of interest to use nano-sized ceramic particles to strengthen the

metal matrix, so-called metal matrix nano-composite (MMNC), while maintaining good ductility. With nanoparticles reinforcement, especially high temperature creep resistance and better fatigue life could be achieved[4,5].

Superior wear resistance is one of the attractive properties in MMCs. It has been found that particulate-reinforced MMCs show wear resistance on the order of 10 times higher than the un-reinforced materials in some load ranges[1]. Many studies have been performed in order to understand the effects of various factors on the wear resistance of conventional MMCs such as the particle size, the fraction of the reinforcing particles, the load, and the sliding speed, on the wear resistance of the particulate-reinforced MMCs with Al matrices[6-8]. The reinforcing particles used in these stud-

Full Paper

ies are mostly SiC or Al_2O_3.

Few investigations were reported on the wear behavior of MMNCs however it is expected that the wear resistance of MMNCs will be higher than the conventional MMCs[9]. In the present investigation the tribological behavior of A356/Al_2O_3 MMNCs were investigated at room and elevated temperatures under dry sliding conditions.

EXPERIMENTAL PROCEDURES

The A356 Al-Si-Mg cast alloy was used as a matrix. The chemical composition of the A356 Al alloy is listed in TABLE 1. Nano-Al_2O_3 particulates were used as reinforcing agents. The Al_2O_3 nano-particulates have two different average sizes, typically, 200 and 60 nm. Several metal matrix nanocomposites (MMNCs) were fabricated with different volume factions of Al_2O_3 nano-particulates such as 1 vol.-%, 3 vol.-% and 5 vol.-%.

TABLE 1 : The chemical composition of A356 alloy.

Alloy	Chemical Composition (wt.-%)						
	Si	Fe	Cu	Mn	Mg	Zn	Al
A356	6.6	0.25	0.11	0.002	0.14	0.026	Bal.

The A356/Al_2O_3 nanocomposites were prepared using a combination of rheocasting and squeeze casting techniques. Preparation of the composite alloy was carried out according to the following procedures: About 1 kg of the A356 Al alloy was melted at 680 ± 2 °C in a graphite crucible in an electrical resistance furnace. After complete melting and degassing by argon gas of the alloy, the alloy was allowed to cool to the semisolid temperature of 602 °C. At such temperature the liquid/solid fraction was about 0.7. The liquid/solid ratio was determined using primary differential scanning calorimeter (DSC) experiments performed on the A356 alloy. A simple mechanical stirrer with three blades made from stainless steel coated with bentonite clay (see Figure 1) was introduced into the melt and stirring was started at approximately 1000 rpm. Before stirring the nano-particles reinforcements after heating to 400 °C for two hours were added inside the vortex formed due to stirring. After that, preheated Al_2O_3 nanoparticles were introduced into the matrix during the agitation. After completing the addition of Al_2O_3 nanoparticles, the agitation was stopped and the mixture was poured into

preheated tool steel mould and immediately squeezed during solidiûcation. Figure 2 shows a photograph of the mould used for squeezing the nanocomposites and the ingot after squeezing. The produced ingot has 30 mm diameter and 130 ± 10 mm length.

Figure 1 : The three blades stainless steel stirrer.

(a) (b)
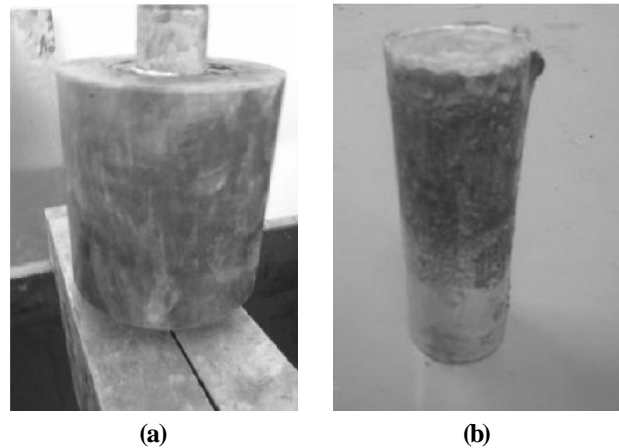
Figure 2 : A tool steel mould used to squeeze the nanocomposites (a) and the ingot after squeezing (b).

The nanocomposites were heat treated at T6 before conducting the machining tests. The nanocomposites were solution treated at 540 ± 1 °C for three hours and then quenched in cold water. After cooling specimens were artificially aged at $160+1$ °C for 12 hours. The micro-hardness was measured on polished samples using the Zwick/Roll micro-hardness tester. The tests were carried out by applying an indentation load of 25 g with a Vickers indenter. Minimum of ten readings were conducted for each specimen and the average value were considered.

Dry sliding wear tests were carried out on the pin-on-disc wear testing machine shown in Figure 3. The elevated temperatures wear tests were performed under dry sliding conditions only up to 250 °C. The wear tests were carried out at room temperature under sev-

eral sliding speeds of 0.4, 0.8 and 1.2 m/s. The load was kept constant at 15 N. The chemical composition of the 314 stainless-steel disc was 0.13 wt% C, 1.8 wt% Si, 21.2 wt% Ni, 24.8 wt% Cr, 1.4 wt% Mn and balance Fe. The wear tests were carried out after heat treating the investigated alloys to T6 condition. The specimens used were of a cylindrical shape having a diameter of 8 mm and a length of 12 mm. The specimen's ends were polished with 1200 grit SiC emery paper and cleaned with acetone. The specimens were then weighted before each experiment on a sensitive balance having sensitivity of 10^{-4} g. The specimen was ûxed on a three jaws clutch. The load was applied to the specimen through a vertical pin fixed with the specimen holder. A ûxed track diameter of 100 mm was used in all tests, and a variable sliding time with an interval of 5 min up to 30 min were applied to conduct the wear tests. The duration of the experiment was controlled by a stopwatch. After each experiment the specimen is weighed again and the weight loss was calculated. For each test condition, at least three runs were performed. The wear rates (the slopes of the sliding time versus cumulative weight loss curves) of the investigated alloys were calculated by using the data after the run-in stage. The elevated temperatures wear tests were performed using an electrical furnace equipped with the wear tester. The furnace was controlled with a control unit to adjust the temperature level. The wear tests were carried out at dry sliding conditions at 100, 150, 200 and 250 °C.

Figure 3 : The pin-on-disc wear tester.

RESULTS AND DISCUSSION

Microstructural examinations

Figure 4 shows example micrographs of the microstructure of the monolithic A356 alloy as well as the A356/Al_2O_3 nanocomposites after heat treatment. It is clear from Figure 4a that the structure of the monolithic A356 Al alloy consists of primary α phase (white regions) and Al-Si eutectic structure (darker regions). Needle-like primary Si particulates were found to be distributed along the boundaries of the α-Al dendrites. Figures 4b and 4c show micrographs of nanocomposites containing 3 vol.-% of Al_2O_3 nanoparticulates having 60 and 200 nm, respectively. Clusters of nanoparticles in the microstructure of the A356/Al_2O_3 nanocomposite were observed. Figure 4d shows high magnification micrograph of Al_2O_3/5 vol.-% (200 nm) nanocomposites. It is clear that clusters of nanoparticles clusters are located inside the α-grains as well as near the eutectic structure. Figure 5a shows high magnification SEM micrograph of the 5 vol.-% Al_2O_3 nanoparticulates (200 nm) showing that nanoparticulates are agglomerating near the Si particles of the eutectic structure. The XRD analysis for the nanoparticles is shown in Figure 5b. Also, it has been observed that increasing the volume fraction of the nanoparticlutes dispersed inside the A356 alloy increases the agglomeration percent. The nanocomposites containing 5 vol.-% exhibited the highest agglomeration percent when compared with those containing 1 and 3 vol.-%.

Porosity measurements indicted that the nanocomposites have porosity content lower than 2 vol.-%. Such low porosity content is attributed to the squeezing process that carried out during the solidification of the nanocomposites. In cast MMCs, there are several sources of gases. The occurrence of porosity can be attributed variously to the amount of hydrogen gas present in the melt, the oxide film on the surface of the melt that can be drawn into it at any stage of stirring, and the gas being drawn into the melt by certain stirring methods[6,11]. Vigorously stirred melt or vortex tends to entrap gas and draw it into the melt. Increasing the stirring time allows more gases to be entered into the melt and hence reduce the mechanical properties.

Full Paper
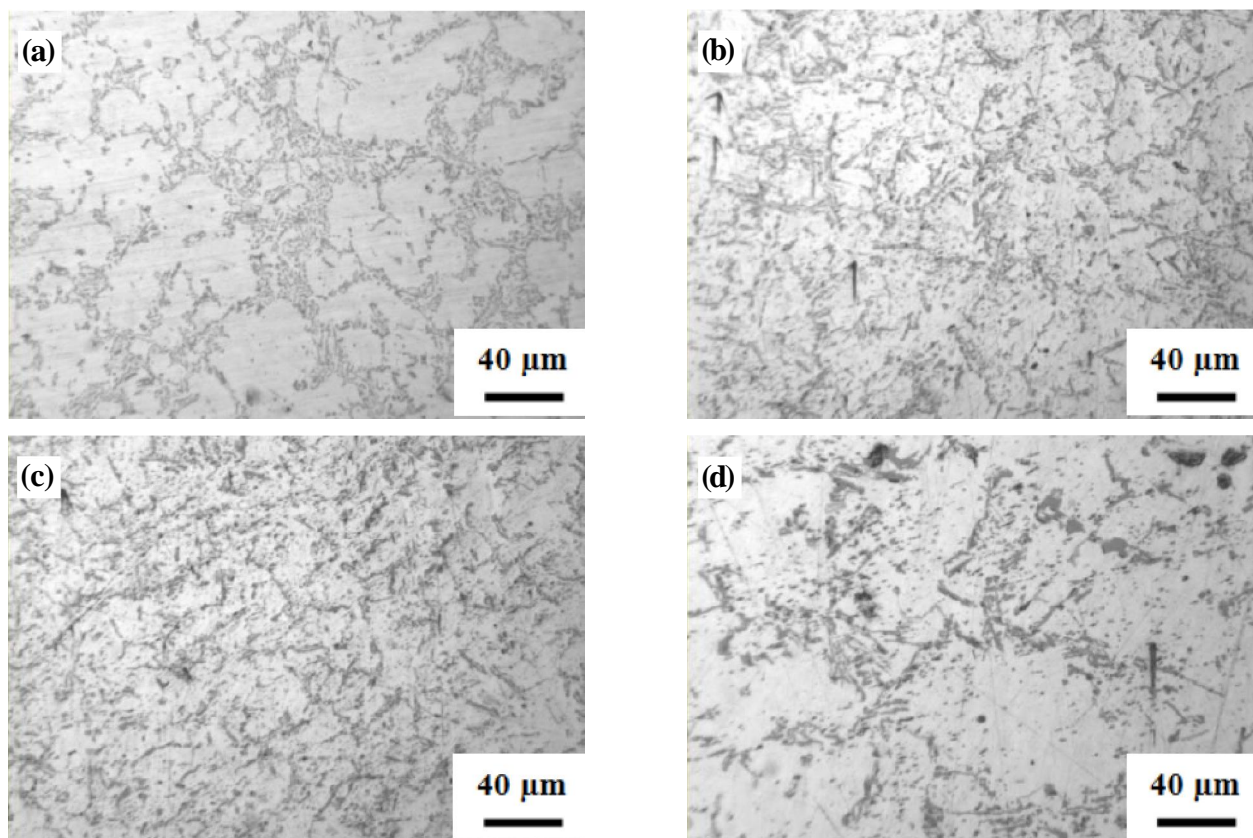
Figure 4 : Optical micrographs for (a) A356 monolithic alloy; (b) A356/3vol.-% Al₂O₃ (60 nm) nanocomposites; (c) A356/3vol.-% Al₂O₃ (200 nm) nanocomposites; (d) A356/5vol.-% Al₂O₃ (200 nm) nanocomposites
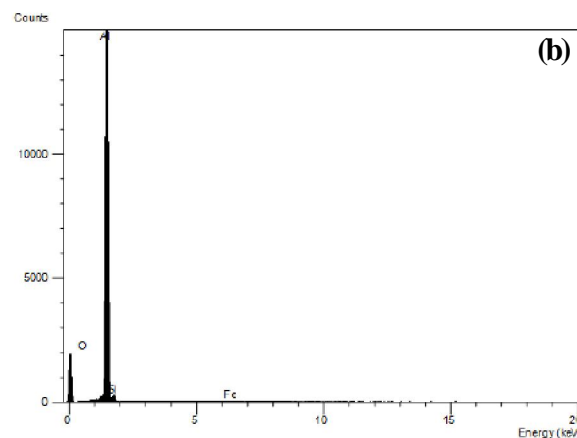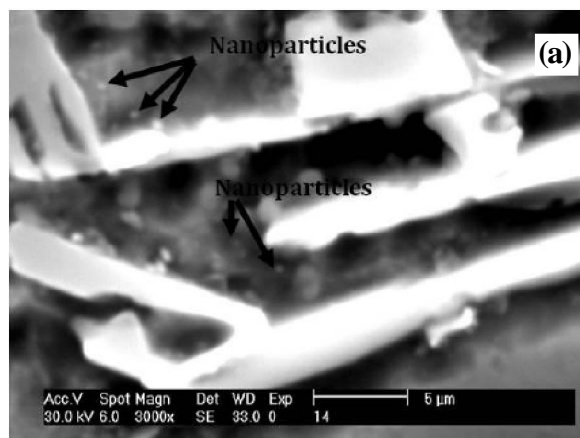
Figure 5 : (a) High magnification SEM micrograph of the 5 vol.-% Al₂O₃ nanoparticulates (200 nm) showing that nanoparticulates are agglomerating near the Si particles of the eutectic structure; (b) XRD analysis for the particles shown in (a).

The amount of liquid inside the semi-solid slurry increases with increasing the temperature which on the other hand reduces the viscosity of the solid/ liquid slurry. Nanoparticles distribution in the A356 Al matrix alloy during the squeezing process depends greatly on the viscosity of the slurry and also on the characteristics of the reinforcement particles them-selves, which inûuence the effectiveness of squeezing in to break up agglomerates and distribute particles. When the amount of liquid inside the slurry is large enough, the particles can be rolled or slid over each other and thus breaking up agglomerations and helping the redistribution of nanoparticles and improving the microstructure.

Microhardness of the nanocomposites

Figure 6 shows the variation of the microhardness of the nanocomposites with the volume fraction of Al_2O_3 nanoparticulates having 60 and 200 nm. It has been found that the nanocomposites exhibited higher average microhardness than the A356 monolithic alloy. The average microhardness of the nanocomposites increases with increasing the volume fraction of the Al_2O_3 nanoparticulates. The nanocomposites containing 200 nm Al_2O_3 nanoparticulates exhibited slightly higher average microhardness when compared with those containing 60 nm Al_2O_3 nanoparticulates. The increase of the hardness of the A356 alloy due to the addition of Al_2O_3 nanoparticulates may attribute to the increase of the resistance to localized plastic deformation.
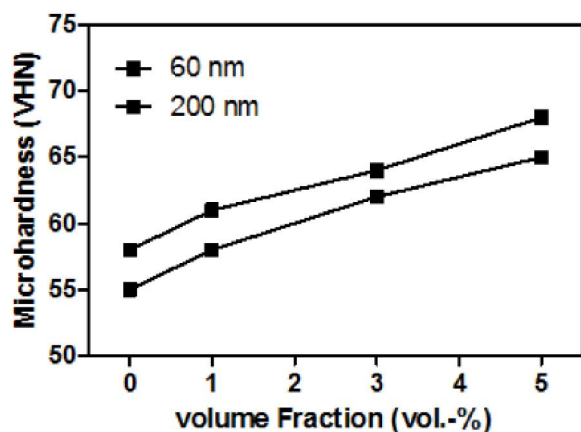
Figure 6 : Variation of the microhardness of the nanocomposites with the volume fraction of Al_2O_3 nanoparticulates.

The increase of the hardness due to the addition of ceramic nanoparticulates to aluminum and magnesium alloys were reported by many workers[4,10,11]. For example, Ansary et al.[11] studied the mechanical properties of A356.1 Al alloy reinforced with nano-sized MgO (50 nm) up to 5vol.-%. The A356.1/MgO nanocomposites were fabricated via stir casting method. The results showed that the hardness of all composites is higher than A356.1 monolithic alloy due to the presence of MgO nanoparticulates with high hardness. The nanocomposites with 5vol.-% content of MgO exhibited lower hardness than samples with 2.5 vol.-% MgO due to the presence of more porosity with the higher content of MgO.

Dry sliding wear behavior of nanocomposites at room temperature

Figure 7 shows the variation of the weight loss with sliding time for different sliding velocity for the A356 monolithic alloy. Figures 8 and 9 show the variation of the weight loss with sliding time for nanocomposites containing 60 nm and 200 nm Al_2O_3 nanoparticulates for different sliding velocities, respectively. The results revealed that the wear loss of the unreinforced alloy and nanocomposites appears to increase with increasing the sliding time. It is noticeable that, at constant applied load, the nanocomposites exhibit lower wear loss compared with the unreinforced alloy. Moreover, it can be seen that the weight loss of the unreinforced alloy and nanocomposites specimens increases with the increase of the sliding velocity. It is clear that mild wear was taken place for both the unreinforced alloy and nanocomposites. Sever wear region was not observed for both the unreinforced alloy and nanocomposites.
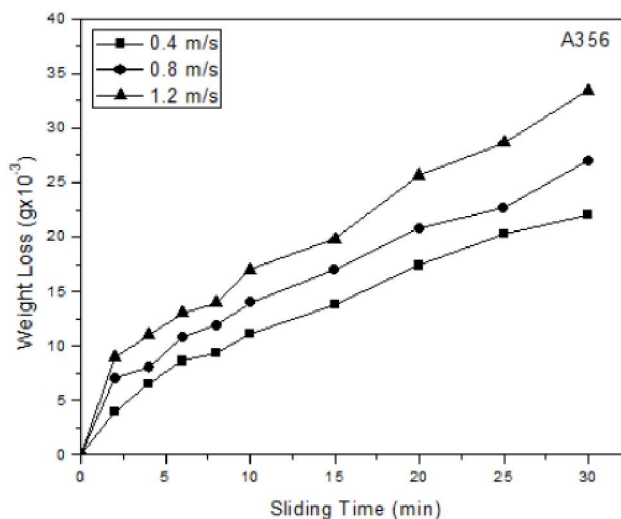
Figure 7 : Variation of the weight loss of the A356 monolithic alloy with sliding time.

Figure 10 shows the variation of the wear rate with sliding velocity for the $A356/Al_2O_3$ nanocomposites containing 60 nm and 200 nm Al_2O_3 nanoparticles. The results showed that, for the unreinforced A356 alloy, increasing the sliding velocity increases significantly the wear rate. While for the $A356/Al_2O_3$ nanocomposites, increasing the sliding velocity increases slightly the wear rates. Such observation was noticed for nanocomposites containing 60 nm and 200 nm Al_2O_3 nanoparticulates. Ithas been found that, at constant sliding velocity and

Full Paper
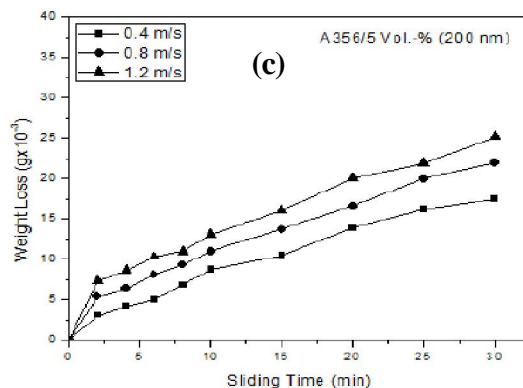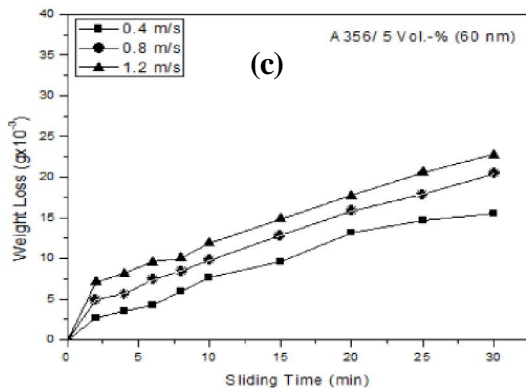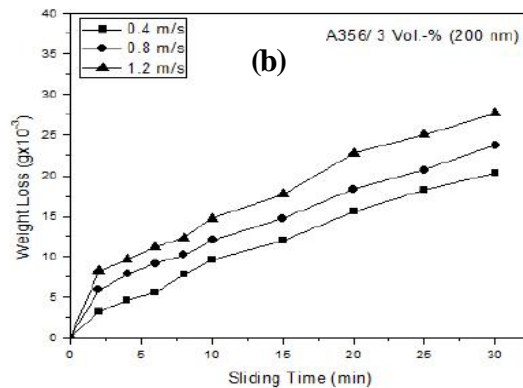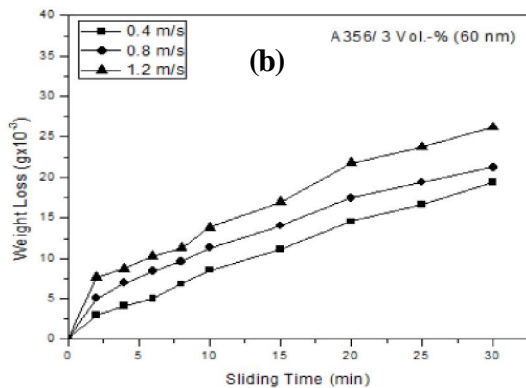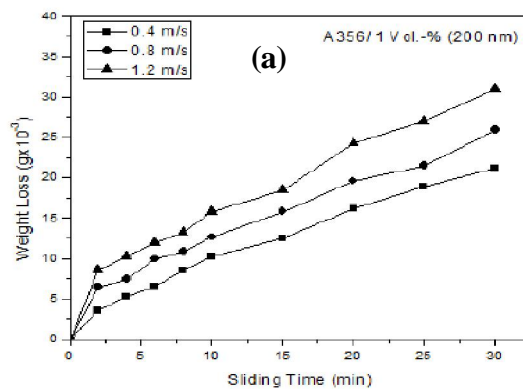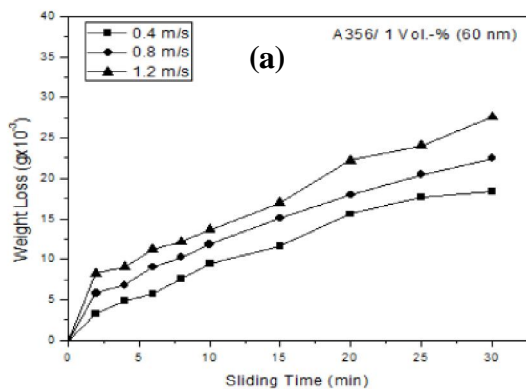
Figure 8 : Variation of the weight loss of the A356/Al₂O₃ (60 nm) nanocomposites with sliding time (a) 1 Vol.-%, (b) 3 Vol.-% and (c) 5 Vol.-%.

Figure 9 : Variation of the weight loss of the A356/Al₂O₃ (200 nm) nanocomposites with sliding time (a) 1 Vol.-%, (b) 3 Vol.-% and (c) 5 Vol.-%.
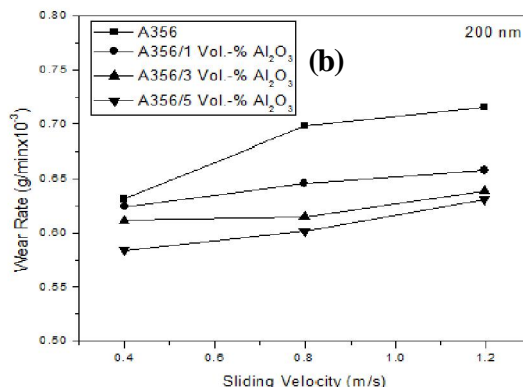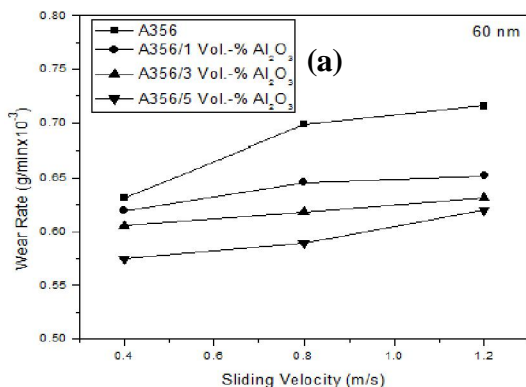
Figure 10 : Variation of the wear rate with sliding velocity for the A356/Al₂O₃ nanocomposites containing (a) 60 nm and (b) 200 nm Al₂O₃ nanoparticles.

Full Paper

volume fraction, the nanocomposites containing 60 nm of Al_2O_3 nanoparticulates exhibited slightly lower wear rates than the nanocomposites containing 200 nm of Al_2O_3 nanoparticulates. At constant nanoparticles size, increasing the volume fraction of the nanoparticulates reduces the wear rates of the nanocomposites.

The above results showed that the wear rate of the A356 alloy was significantly improved by the addition of the Al_2O_3 nanoparticulates. The wear rate of the nanocomposites was reduced to about 25% (for nanocomposites containing 5 vol.-% of nanoparticulates) of the wear rate of the A356 monolithic alloy. The wear rate of the nanocomposites was slightly influenced by increasing the sliding velocity. In contrast, wear rate of the unreinforced A356 alloy was significantly influenced by the sliding velocity. The wear rate of the nanocomposites was reduced by increasing the volume fraction and/or reducing the Al_2O_3 nanoparticles size. For any given nanoparticles content, said 1 vol.-%, the mean distance between neighboring nanoparticles for the nanocomposite with smaller filler particles (as in 60 nm nano-sized particles) was smaller than that with the bigger particles (200 nm nano-sized particles). For, example, the number of the nanoparticles per unit volume for the nanocomposite with 60 nm Al_2O_3 nanoparticles would be greater than that of the composite with the 200 nm Al_2O_3 nanoparticles. As the nanoparticles were uniform sized spherical particles, the greater the number of the particles on the worn surface, the larger the contact area between the particles and the contact disc, and hence the better the wear resistance offered by the Al_2O_3 nanoparticles. That might be a reason for explaining the better improvement of the wear resistance by using nanoparticles.

Figures 11 and 12 show optical photographs of the worn surfaces of the A356 unreinforced matrix and the A356/Al_2O_3 nanocomposites, respectively, after dry sliding against stainless steel disc for 30 min at sliding velocity of 1.2 m/s and applied load of 15 N. It is clear that more surface damage is noticed on the surface of the A356 unreinforced alloy. Large ploughing areas could be seen in the worn surface of the unreinforced A356 alloy. This means that an extensive surface damage due to the high material removal (delamination process) rate takes place in the A356 monolithic alloy. The appearance of the exten-

sive deformed worn surface of the A356 unreinforced matrix alloy suggests softening of the matrix.
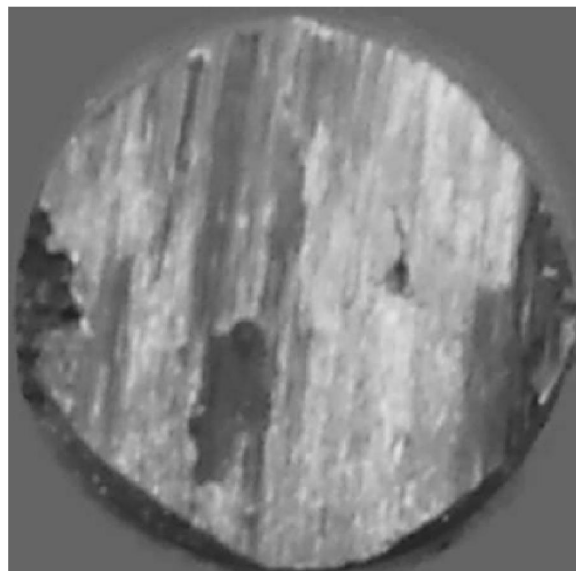
Figure 11 : Optical micrograph of the worn surface of the A356 unreinforced matrix after dry sliding for 30 min at sliding velocity of 1.2 m/s.

From photographs shown in Figure 12, it was observed that numerous craters are present over the entire wear track. It has been noticed for the nanocomposites that, the extent of grooving in the worn surfaces of the composites is reduced with increased content of Al_2O_3 indicating lower material removal as evidenced in photographs shown in Figure 12. With increase in volume fraction and/or reducing the size of the Al_2O_3 nanoparticulates, the worn surface was more uniform i.e. less number of craters is observed. Presence of craters in the worn surface is believed to be due to the cracking and breaking of delaminated layer into fragments.

The reduction of the wear rate of the A356 alloy due to the addition of Al_2O_3 nanoparticulates may attribute also to the increase of the hardness of the nanocomposites compared with the A356 unreinforced matrix. Increasing the volume fraction of the nanoparticulates increases the hardness of the nanocomposites and hence reduces the wear rate of the nanocomposites. The adhesive wear theory stated by Archard[8] defined wear volume as a function of sliding speed, normal load and material hardness. This theory was based on a mechanism of adhesion at the asperities and the material removal process was re-

Full Paper

lated to a cohesive failure of asperities. The processes of crack nucleation and subsequent growth were disregarded. With the assumption that wear particles could be described as hemispherical particles of the same radius as the contact area, Archard developed the following expression for wear rate, W (volume of material worn):

$$W = \frac{KdP}{3H} \qquad (1)$$

where K = wear coefficient, d = sliding distance, P = applied normal load and H = bulk hardness of the material. *Archard* concluded that the wear rate was proportional to the applied load (assuming that the average size of the contact areas and the wear particles were constant) and that the wear rate was independent of the apparent area of contact. The theory predicted that enhanced wear resistance was associated with increase in hardness.
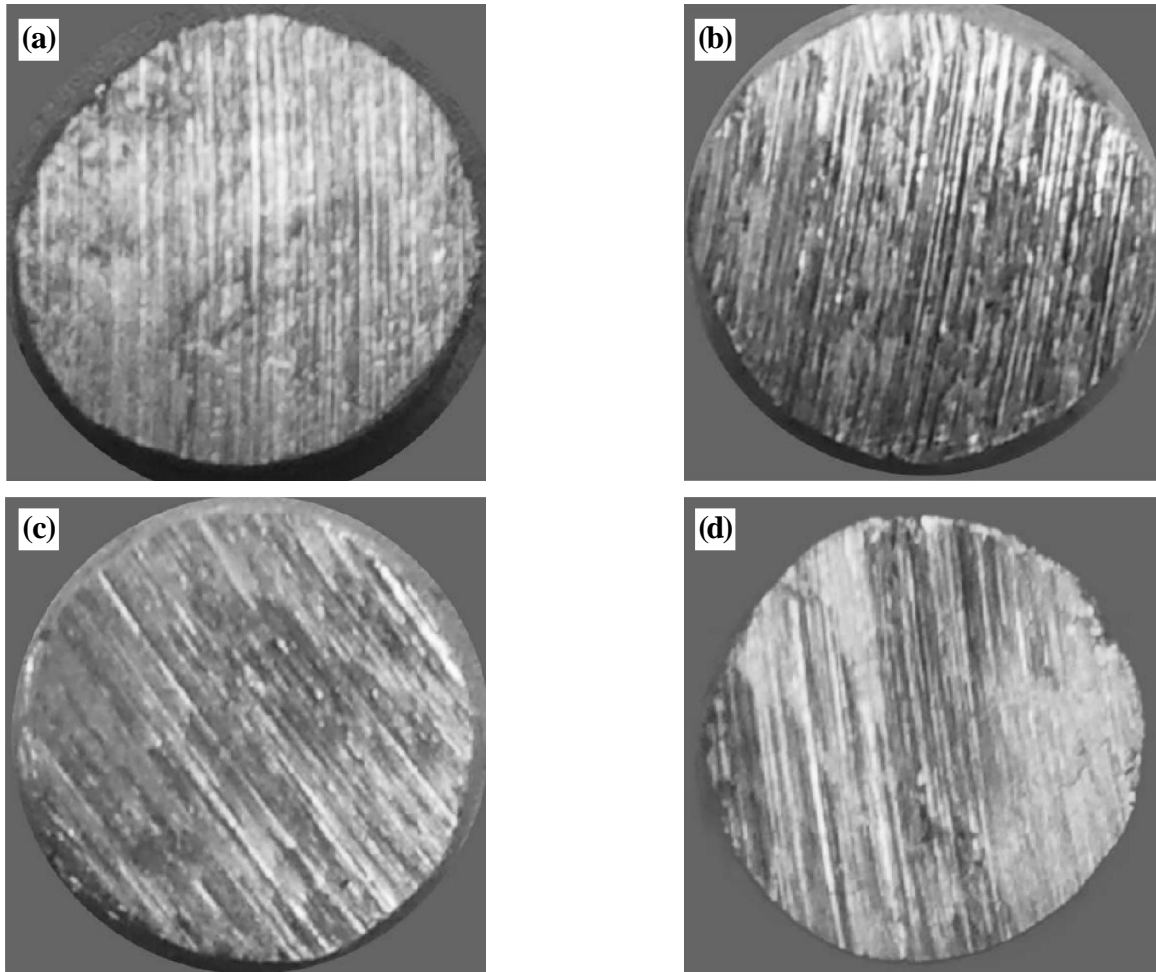
Figure 12 : Optical micrograph of the worn surface of the A356/Al₂O₃ nanocomposites after dry sliding for 30 min at sliding velocity of 1.2 m/s. (a) 1 Vol.-% 60 nm, (b) 1 vol.-% 200 nm, (c) 5 vol.-% 60 nm (d) 5 vol.-% 200 nm nanocomposites.

Suh[12] proposed that at low sliding speeds, wear debris formation could be described by a delamination wear theory. Wear processes such as adhesive wear, fretting and fatigue were all related to this same mechanism. Suh[12] stated that wear occurred by the following sequential steps: (1) Cyclic plastic deformation of surface layers by normal and tangential loads, (2) Crack or void nucleation in the deformed layers at inclusions or second-phase particles, (3) Crack growth nearly parallel to the surface, and (4) Formation of thin, long wear debris particles and their removal by extension of cracks to the surface. The rate-determining mechanism of wear showed dependence on the metallurgical structure. When sub-surface deformation controlled the wear rate, hardness and fracture toughness were both considered to be major influencing factors.

In a study of dry sliding wear of dispersion-hardened alloys, delamination wear theory was identified as

Full Paper

a major wear process[13]. Hardness and friction coefficient played a major role in the overall wear process. The wear resistance decreased with increased volume fraction of the oxide phase, even when hardness was increased. Crack propagation was considered to be the wear-rate controlling factor. Cracks were initiated at the particle/matrix interface or by fracture of the particles. For crack nucleation at particle/matrix interfaces, the following conditions were necessary: (1) Tensile stress across the interface should exceed the interfacial bond strength and (2) Elastic strain energy released upon decohesion of the interface should be sufficient to account for the surface energy of the crack created.

Investigations showed that for second phase particles to be a significant factor in the nucleation of a void or micro-crack, they must possess a diameter in excess of 2.5 µm in order to satisfy the energy conditions. Therefore, for good wear resistance it was found to be desirable to have an alloy reinforced with a large volume fraction of very small coherent particles[14]. The nanoparticles have high surface area to volume ratio which increase the coherency and hence improves the wear resistance of the alloys.

It is believed that the reduction of the wear rate in nanocomposites is lower also because of the presence of the hard Al_2O_3 layers within the tribolayer. The lower wear rates in $A356/Al_2O_3$ nanocomposites compared with the A356 unreinforced alloy reduces the shear stresses transmitted to the bulk subsurface material underneath the tribolayer, which is one of the possible reasons as to why mild wear regime tends to higher loads, and velocities without the removal of the tribolayers.

The wear behavior of Al-based metal matrix nanocomposites (MMNCs) was investigated by many workers[9,15,16]. The improvement of the wear resistance of the Al matrix was reported by the workers. For example, Debdas et al.[16] examined the wear behavior of Al/Fe_2O_3 MMNCs fabricated using in-situ technique. The wear experiments were performed in the gross slip fretting regime to understand their tribological properties against bearing steel in the ambient conditions of temperature (22–25 °C) and humidity (50–55%RH). For unreinforced Al, extensive plastic deformation was observed to cause more wear. The deformation induced wear is explained on the basis of formation of persis-

tent slip bands and subsequent cracking as a result of cyclic deformation during large number of fretting cycles. The improvement in hardness due to harder aluminide reinforcements causes increase in wear resistance of 20 vol.% reinforced composite and this has observed to lead better wear resistance. For 40 vol.% reinforcement, a transition in wear mechanism from predominantly abrasion and deformation to predominant abrasion and tribochemical wear takes place. This contributed to larger wear loss in the composites with 40 vol.% in-situ reinforcement.

The tribological behavior of Al/Mg alloys reinforced with CNTs was studied by Sheng-Ming et al.[9]. The MMNCs were fabricated by pressureless infiltration process. The friction and wear behaviors of the composite were investigated using a pin-on-disk wear tester under unlubricated condition. The tests were conducted at a sliding speed of 0.1571 m/s under an applied load of 30 N. Within the range of CNTs volume fraction from 0% to 20%, the wear rate of the composite decreased steadily with the increase of CNTs content in the composite. The favorable effects of CNTs on wear resistance are attributed to their excellent mechanical properties, being well dispersed in the composite and the efficiency of the reinforcement of CNTs. SEM examinations of the worn surfaces of MMNCs showed that, during the steady-state wear process, the oxidation wear was found to be the main wear-mechanism for the CNTs reinforced Al composites.

Elevated temperatures wear behavior at elevated temperatures

The variation of the wear rate of the unreinforced Al matrix as well as $A356/Al_2O_3$ with the test temperature, at different sliding speeds, is shown Figure 13 to Figure 15. The results showed that the wear rate of the unreinforced Al matrix was increased significantly after 150 °C. Increasing the sliding speed and temperature increases the wear rate of the nanocomposites. The wear resistance of the nancomposites increases with increasing the volume fraction and/or reducing the size of the Al_2O_3 nanoparticulates. Both unreinforced Al matrix and the composites show mild (at low temperatures) and severe (at high temperatures) wear regimes. The transition from mild to severe wear depends on sliding speed, test temperature and the volume fraction and

Full Paper

size of Al_2O_3 nanoparticulates. However, the test temperature has the greatest influence on the transition temperature than other mentioned parameters. Moreover, the transition temperature increases with increasing the volume fraction and/or reducing the size of the Al_2O_3 particulates. The composites exhibited transition temperature between 150 and 200 °C, while the unreinforced alloy exhibited a transition temperature between 100 and 150 °C. The decrease of the wear resistance of the composites due to the increase of the test temperature is attributed to the decrease of the strength of the composites at elevated temperatures.
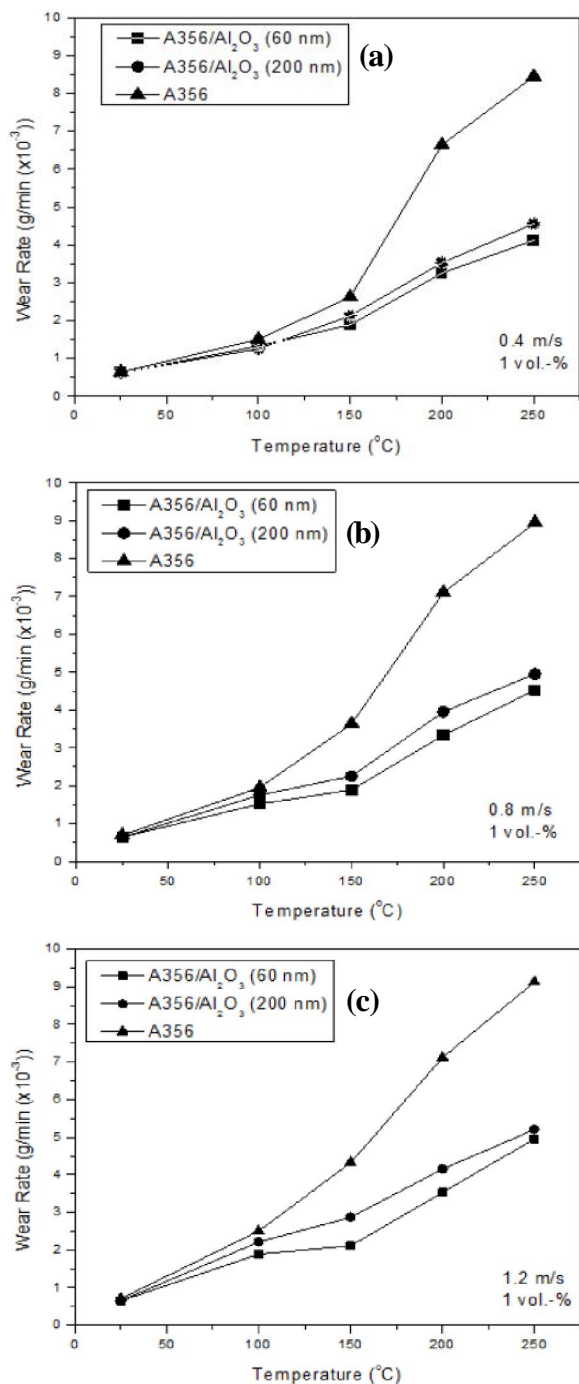
Figure 13 : Variation of the wear rate with the temperature for A356/Al₂O₃ nanocomposites containing 1 vol.-% of Al₂O₃ nanoparticles at sliding speeds of (a)0.4 m/s, (b) 0.8 m/s and (c) 1.2 m/s.
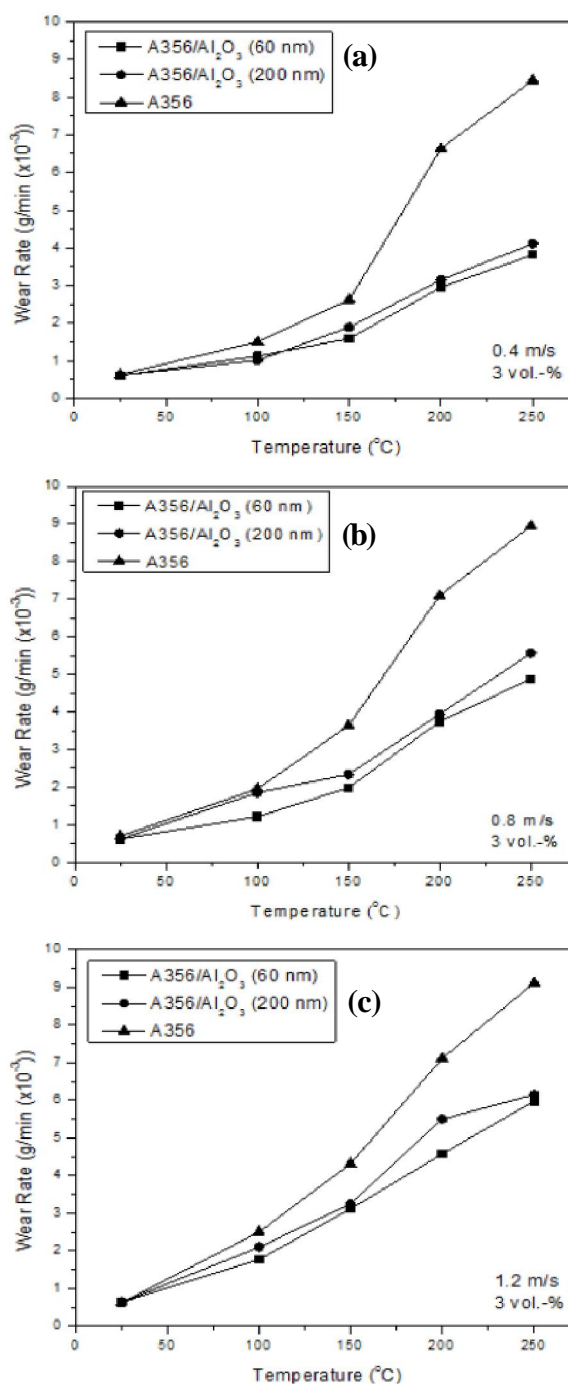
Figure 14 : Variation of the wear rate with the temperature for A356/Al₂O₃ nanocomposites containing 3 vol.-% of Al₂O₃ nanoparticles at sliding speeds of (a)0.4 m/s, (b) 0.8 m/s and (c) 1.2 m/s.

For the Al unreinforced matrix and the nanocomposites, wear tests performed at temperatures below the transition temperature produced relatively smooth worn surfaces. SEM examinations of the worn surface of the nanocomposites showed that the worn surfaces were partially covered with layers of iron oxide (see Figure 16). The iron oxides can act as solid lubricants and expected to reduce the wear rates with temperature.
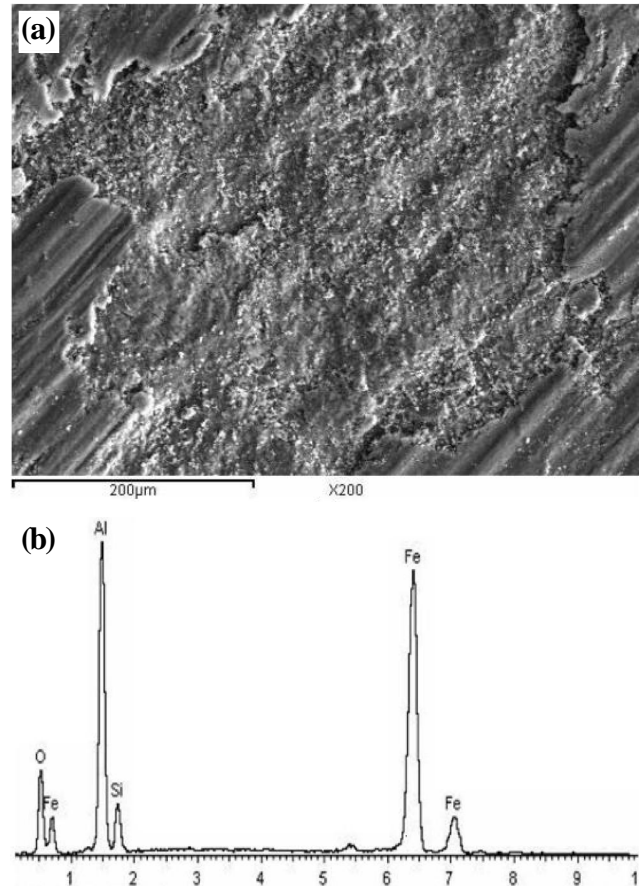
Figure 16 : (a) SEM micrograph shows the formation of the iron oxide layer on the worn surface of A356/5 vol.-% 60 nm Al₂O₃ nanocomposites (b) EDX analysis of the oxide layer.

The oxide layers (tribolayer) at the contact surfaces were formed as a result of the iron transferred from the counterface due to the high compressive stresses developed at the interfaces. The compacted tribolayer is harder than the bulk material. During sliding metal–metal wear tests of the nanocomposites, the iron oxide layer formed on the contact surfaces acted as a solid lubricant and improved wear resistant. The formation of the tribolayers increased the surface hardness signiûcantly and played an important role in delaying the mild-to-

Figure 15 : Variation of the wear rate with the temperature for A356/Al₂O₃ nanocomposites containing 5 vol.-% of Al₂O₃ nanoparticles at sliding speeds of (a)0.4 m/s, (b) 0.8 m/s and (c) 1.2 m/s.

Full Paper

severe wear transition in aluminum matrix nanocomposites. The presence of Al$_2$O$_3$ nano-particles served as a safeguard by generating a hard compacted tribolayer with smooth surface and sufûcient thickness to protect the material underneath from excessive sub-surface damage by forming a physical barrier of about 10 to 50 µm thick with the counterface.

At test temperatures above the transition temperature, the observations indicated that the severe wear of both Al and Al/Al$_2$O$_3$ composites, took place by material transfer to the counterface. The thermal softening due thermal heating increased the transfer rate of the matrix material to counterface material. The severe wear at elevated temperatures is influenced by the mechanical properties of the matrix. The presence of secondary reinforcement particulates as well as the tribolayer appears to retard the extent of the plastic deformation imposed on the wearing matrix subjected to elevated temperatures. This explains the high mild-severe wear transition temperature of the composites compared with the monolithic matrix. Straffelini et al.[17] showed that at elevated temperatures and at constant SiC particles size, the thickness of the tribolayer depends on the volume fraction of the ceramic particles. They explained that by dynamic phenomena which responsible for the surface damage of the composites: (1) abrasive grooving made by the hard particles in the counterface and (2) the transfer from the counterface material. In the present investigation, the composites containing 5 vol.% of 60 and 200 nm Al$_2$O$_3$nanoparticulates, offered greater resistance to grooving and the rate of transfer of the counterface material is high is thus sufficient high to allow formation of a thick tribolayer, which protect the underlying material. While in case of composites containing 1 vol.-% of 60 and 200 nm Al$_2$O$_3$ nanoparticulates, abrasive grooving predominate because of its lower hardness and the rate of transfer is not sufficient to form a thick tribolayer.

However several investigations were carried out to study the tribological behavior of Al based MMCs at room temperature[1,2,6,7], only limited investigations on the bebaviour of Al-based MMCs at elevated temperatures were reported[18-22]. This is very surprising especially when it is considered that elevated temperatures are often found in industrial applications. Typical examples are piston liners and cylindrical heads of automobile engines, as well as brake rotors. Singh and Alplas[18] studied the elevated temperatures wear behavior of Al6061-20% Al$_2$O$_3$

MMC. The results showed that both Al6061 alloy and the particulate reinforced Al606l-20% Al$_2$O$_3$ composite show a mild to severe wear transition when the surrounding temperature is increased above a certain temperature. This transition occurs at higher temperatures in the composite. The same observation was noticed by Kumar et al.[22] when the AA6061/fly-ash MMCs were investigated. The results had shown transition from mild-to-severe wear for unreinforced alloy in the temperature range of 200–300 ºC. With the addition of ûy ash to AA6061, the mild-to-severe wear transition was not noticed even up to 300 ºC. In the current investigation, the same observation was also noticed. The A356/Al$_2$O$_3$ nanocomposites exhibited mild-to-sever wear transition temperature between 150 and 200 ºC, while the A356 Al alloy between 100 and 150 ºC.

CONCLUSIONS

According the results obtained in the fourth stage of the current project, the following conclusions can be pointed out:

1. The A356/Al$_2$O$_3$ nanocomposites exhibited higher wear resistance at both room and elevated temperatures when compared with the A356 monolithic alloy. Increasing the volume fraction and/or reducing the Al$_2$O$_3$ nanoparticles size improves the wear resistance of the A356/Al$_2$O$_3$ nanocomposites.
2. The nanocomposites exhibited transition temperature between 150 and 200 ºC, while the unreinforced alloy exhibited a transition temperature between 100 and 150 ºC.
3. Examinations of the worn surface of the nanocomposites showed that the worn surfaces were partially covered with layers of iron oxide. The iron oxides can act as solid lubricants and expected to reduce the wear rates with temperature.

ACKNOWLEDGEMENTS

Full Paper

Sihimi Director of the research center of Excellency at KKU and Dean of the faculty of Science and finally great thanks to Dr. Khaled Al-Zailaie, Dean of the faculty of engineering at KKU, for their support.

REFERENCES

[1] ASM handbook; Composites, ASM International, **21**, **(2001)**.

[2] Nikhilesh Chawla, Krishan K.Chawla; 'Metal matrix composites', Springer Science and Business Media Inc., **(2006)**.

[3] I.S.El-Mahallawi, K.Eigenfield, F.Kouta, A.Hussein, T.S.Mahmoud, R.M.Ragaie, A.Y.Shash, W.Abou-Al-Hassan; 'Synthesis and characterization of new cast $A356/(Al_2O_3)_P$ metal matrix nano-composites', ASME, In the proceeding of the 2nd Multifunctional nanocomposites & nanomaterials: International conference & exhibition, organized by the American University in Cairo - AUC, in collaboration with Cairo University, Sharm El Sheikh, Egypt, January 11-13, **(2008)**.

[4] Jie Lan, Yong Yang, Xiaochun Li; Microstructure and microhardness of SiC nanoparticles reinforced magnesium composites fabricated by ultrasonic method, Mater.Sci.Eng.A, **386**, 284-290 **(2004)**.

[5] M.Habibnejad-Korayem, R.Mahmudi, W.J.Poole; Enhanced properties of Mg-based nano-composites reinforced with Al_2O_3 nano-particles, Mater.Sci.Eng.A, **519**, 198-203 **(2009)**.

[6] M.Abdel-Aziz, Z.I.Zaki, A.M.Gaafer, T.S.Mahmoud; Mechanical and wear characteristics of Al_2O_3 and TiC particulate reinforced AA6063 Al alloy hybrid composites, In 12th European conference on composite materials, Biarritz, France, 29 August-1 September, **(2006)**.

[7] T.S.Mahmoud; Tribological characteristics of A390/ Gr_p MMCs fabricated using a combination of rheocasting and squeeze casting techniques, Proc.IMechE, Part C: J.Mech.Eng.Sci., **222(C2)**, 257-266 **(2008)**.

[8] C.Subramanian; Some considerations towards the design of a wear resistant aluminium alloy, Wear, **155**, 193-205 **(1992)**.

[9] Sheng-Ming Zhou, Xiao-Bin Zhang, Zhi-Peng Ding, Chun-Yan Min, Guo-Liang Xu, Wen-Ming Zhu; Fabrication and tribological properties of carbon nanotubes reinforced Al composites prepared by pressureless infiltration technique, Composites: Part A, **38**, 301-306 **(2007)**.

[10] M.Habibnejad-Korayem, R.Mahmudi, W.J.Poole; Enhanced properties of Mg-based nano-composites reinforced with Al_2O_3 nano-particles, Mater.Sci.Eng.A, **519**, 198-203 **(2009)**.

[11] A.Ansary Yar, M.Montazerian, H.Abdizadeh, H.R.Baharvandi; Microstructure and mechanical properties of aluminum alloy matrix composite reinforced with nano-particle MgO, Journal of Alloys and Compounds, **484**, 400-404 **(2009)**.

[12] N.P.Suh; The delamination theory of wear, Wear, **25**, 111-124 **(1973)**.

[13] N.Saka, J.J.Pamies-Teixeira, N.P.Suh; Wear of two-phase metals, Wear, **44**, 77-86 **(1977)**.

[14] N.Saka, N.P.Suh; Delamination wear of dispersion-hardened alloys, Trans.ASME, Ser.B, J.Engng.Indust., **99**, 289-294 **(1977)**.

[15] A.Shafiei-Zarghani, S.F.Kashani-Bozorg, A.Zarei-Hanzaki; Microstructures and mechanical properties of Al/Al_2O_3 surface nano-composite layer produced by friction stir processing, Materials Science and Engineering A, **500**, 84-91 **(2009)**.

[16] Debdas Roy, Bikramjit Basu, Amitava Basu Mallick, B.V.Manoj Kumar, Sumit Ghosh; Understanding the unlubricated friction and wear behavior of Fe-aluminide reinforced Al-based in-situ metal–matrix composite, Composites: Part A, **37**, 1464-1472 **(2006)**.

[17] G.Straffelini, M.Pellizzari, A.Molinari; Influence of load and temperature on the dry sliding behavior of Al-based metal matrix composites against friction material, Wear, **256**, 754-763 **(2004)**.

[18] J.Singh, A.T.Alpas; Elevated temperature wear of Al6061 and Al6061-20%Al_2O_3, Scripta Metallurgica et Materialia, **32(7)**, 1099-1105 **(1995)**.

[19] S.M.R.Mousavi Abarghouie, S.M.Seyed Reihani; Investigation of friction and wear behaviors of 2024 Al and 2024 Al/SiC_p composite at elevated temperatures, Journal of Alloys and Compounds, **501**, 326-332 **(2010)**.

[20] S.Kumar, V.Subramanya Sarma, B.S.Murty; High temperature wear behavior of Al–4Cu–TiB_2 in situ composites, Wear, **268**, 1266-1274 **(2010)**.

[21] S.Wilson, A.T.Alpas; Effect of temperature on the sliding wear performance of Al alloys and Al matrix composites, Wear, **196**, 270-278 **(1996)**.

[22] P.R.S.Kumar, S.Kumaran, T.Srinivasa Rao, S.Natarajan; High temperature sliding wear behavior of press-extruded AA6061/fly ash composite, Materials Science and Engineering A, **527**, 1501-1509 **(2010)**.